11.5

Multiple Scattering in Thick Multifractal Clouds

B. P. Watson[1]*, S. Lovejoy[2], Y. Grosdidier[2], D. Schertzer[3]

[1]Department of Physics, St. Lawrence University, Canton, NY 13617 USA
[2]Department of Physics, McGill University, 3600 University St., Montreal, Que., Canada
[3]CEREVE, Ecole Nationale des Ponts et Chaussées, 6-8, avenue Blaise Pascal, Cité Descartes, 77455 MARNE-LA-VALLEE Cedex, France

ABSTRACT

Satellite studies have shown that cloud radiances (at both visible and infra red wavelengths) are scale invariant over scales spanning much of the meteorologically significant range, and airborne lidar data have shown that vertical cross sections of passive scalar clouds are also scaling but with quite different exponents in the horizontal and vertical directions.

Over the last twenty years, many studies have been made of radiative transfer in scaling cloud fields, the vast majority of which have been limited to numerical studies in fairly optically thin clouds. An exception to this was the development of a formalism for treating single scattering in optically thick but conservative multifractal clouds without significant holes. In this paper we show how these results can be extended to non conservative and general "universal" multifractal clouds dominated by «Lévy holes», and how the analytic single scattering results can be generalized to multiple scattering including for very thick clouds. These theoretical multiple scattering predictions are numerically tested using the discrete angle radiative transfer (DART) approach in which the radiances decouple into non-interacting families with only four (for 2-D clouds) radiance directions each. Sparse matrix techniques allow for rapid and extremely accurate solutions for the transfer; the accuracy is only limited by the spatial discretization.

By "renormalizing" the cloud density, we relate the mean transmission statistics to those of an equivalent homogeneous cloud. Since the numerics on the special DART phase functions accurately validate a phase function independent theory the basic results will be valid for any phase function. For realistic clouds (α=1.75, C_1=0.1, H=0.33, 1-g=0.15) and optical thickeness of 100, we predict a 30-40% higher transmission when compared to the plane parallel predictions.

*Corresponding author: Department of Physics, St. Lawrence University, Canton NY 13617
e-mail: bwatson@stlawu.edu

1. INTRODUCTION

1.1 Overview

Clouds – both meteorlogical and astrophysical – and their associated radiation fields are highly variable over huge ranges of space-time scales. An understanding of both the variability and the inter-relation between the two fields is of fundamental importance in meteorology, climatology, and astrophysics. The relation between radiation fields and the associated scatter density fields is also a challenging problem in the physics of disordered media (sporting many novel statistical features). This problem generally arises in systems with temporal and spatial variability originating in turbulent-like phenomena and is therefore ubiquitous.

Since the variability is a consequence of turbulent atmospheric or magneto-turbulent astrophysical dynamics which span huge ranges of scale, the natural framework is scaling fields, *i.e.,* multifractals. Indeed, in the atmosphere direct measurement of nearly 1000 satellite based cloud radiances spanning the scales of kilometers to thousands of kilometers has shown that the radiance fields are multifractal with deviations less than 1% per octave in scale ([*Lovejoy et al.*, 2001], [Lovejoy, 2005 #826]). In this framework, the various cloud morphologies and types are simply manifestations of anisotropic (but still scaling) multifractal generating mechanisms. In astrophysical systems, scaling has been observed from planetary and stellar scales, up to interstellar and even galactic scales (e.g. [Witt & Gordon, 1996], [Varosi & Dwek, 1997], [Juvela, 1997], [Witt & Gordon, 2000], [Acker, et al., 2002], [Grosdidier & Acker, 2004], and references therein).

Similarly, most astrophysical plasmas appear to be manifestations of magneto-hydrodynamical turbulence and are modeled by turbulent fragmentation processes. Many studies were indeed devoted to characterize the monofractal nature of several astrophysical density or velocity fields (e.g. [*Bazell & Désert*, 1988], [*Beech*, 1992], [*Blacher & Perdang*, 1990], [*Gill & Henriksen*, 1990], [*Falgarone, et al.*, 1991], [*Miesch & Bally*, 1994], [*Brunt & Heyer*, 2002], [*Falgarone, et al.*, 2004], and references therein). More recently, the multifractal nature of the intermittency has been recognized because intermittency affects many chemical reactions and, more generally, because it has a profound impact on structure formation (*e.g.,* [*Falgarone, et al.*, 2004], [*Grosdidier & Acker*, 2004], and references therein). Hence, as in terrestrial clouds, one is lead to adopt the multifractal approach in order to best describe astrophysical cloud morphologies and dynamics. Finally, there is also a strong need for quantitative results of radiative transport in astrophysical plasmas since most (if not all) of the information obtained from distant astrophysical sources is in the form of electromagnetic radiation. Note, however, that the magneto-hydrodynamical turbulence observed in some nebulae or giant molecular clouds (apparently supersonic) are different from atmospheric turbulence ([*Fleck*, 1996], [*Gill & Henriksen*, 1990]), notably the scaling anisotropic vertical stratification of the latter ([Schertzer & Lovejoy, 1985], [Lilley et. al., 2004]). The large compressibility of the nebular gases and the possible multiplicity of turbulence energy sources are likely the main explanations for that difference.

In this paper, we focus on the theoretically well-defined problem of radiative transport in multifractal media. There are two parts to the problem each with corresponding model choices. The first is for the cloud/medium, the second is for the transfer. For simplicity, we will limit our attention to isotropic (self-similar) multifractals, and to multifractals with stable, attractive generators: the "universal multifractals". As for the choice of transport model, we opt for the traditional radiative transfer equation but with a special choice of scattering phase function such that scattering only occurs through a discrete set of angles. This makes the theory and numerics particularly simple ([*Lovejoy, et al.*, 1990], [*Gabriel, et al.*, 1990], [*Davis, et al.*, 1990]) without modifying the basic statistical properties of the transport (the scaling exponents). The slightly simpler transport problem of diffusion on multifractals ([*Meakin*, 1987],[*Lovejoy, et al.*, 1998], , [*Weissman & Havlin*, 1988], [*Lovejoy, et al.*, 1993], [*Marguerite, et al.*, 1997]) is itself quite interesting, but (except in 1-D, [*Lovejoy, et al.*, 1993], [*Lovejoy, et al.*, 1995]) is not in the same universality class as radiative transport ([*Lovejoy, et al.*, 1990]). It could be mentioned that much of the work on transport in scaling media has focused on binary systems in which the medium is modeled as a geometric set of points (e.g. the problem of electrical conduction in a conducting percolating system, see the reviews [*Havlin & Ben-Avraham*, 1987] [*Bouchaud & Georges*, 1990]); the corresponding fractal sets are simpler than the multifractal measures relevant to turbulence.

1.2 External horizontal variability, and fractal models

The theory of radiative transfer in plane parallel horizontally homogeneous (1-D) media is elegant and general ([*Chandrasekhar*, 1950]). For horizontally inhomogeneous media there is no consensus on the appropriate model, nor is the transport problem tractable analytically. For these reasons the use of 1-D models long dominated the field: in fact, the effect of horizontal variablity was both underestimated and neglected. On the occasions where horizontally inhomogeneity was considered at all, it was usually reduced to the inhomogeneity of the external cloud/medium boundary (e.g. cubes, spheres, cylinders, e.g. [*Busygin, et al.*, 1973], [*McKee & Cox*, 1976], [*Preisendorfer & Stephens*, 1984] with the internal field still being considered homogeneous. When internal horizontal inhomogeneity was considered it was typically confined to narrow ranges of scale so that various transfer approximations could be justified, see e.g. [*Weinman & Swartzrauber*, 1968], [*Welch, et al.*, 1980].

Motivated by the explosion of interest in scaling systems and the realization that many geophysical systems (including clouds) were scaling over large ranges, the first studies of radiative transport on fractal systems appeared (e.g. [*Gabriel*, *et al.,* 1986], [*Cahalan*, 1989], [*Lovejoy & Schertzer*, 1989], [*Lovejoy et al.*, 1990], [*Gabriel, et al.,* 1990], [*Davis, et al.*, 1990], [*Barker and Davies*, 1992], [Cahalan, 1994 #854; Cahalan, 1994 #95]). These works used various essentially academic fractal models and focused on the (spatial) mean (i.e., bulk) transmission and reflectance. They clearly showed that i) fractality generally leads to non classical ("anomalous") thick cloud scaling exponents, ii) the latter were strongly dependent on the type of scaling of the medium, and iii) they are independent of the phase function ([*Lovejoy, et al.*, 1990]).

By the 1990's, it was clear that scaling generically leads to multifractal fields and that clouds were – as expected for turbulent fields – more nearly multi- than mono- fractal ([*Gabriel, et al.*, 1988], [*Lovejoy and Schertzer*, 1990]). This pointed to the importance of understanding transport in the more realistic multifractal systems. Since the generic multifractal process is the multiplicative cascade, this leads to transport studies on cascade based cloud models. The two classes of cloud model which have been used for this purpose are the fractionally integrated flux model (FIF, [*Schertzer & Lovejoy*, 1987]) and the bounded cascade model [*Cahalan*, 1994]. In the FIF model, a multiplicative cascade generates a (scale by scale) conservative multifractal (for example, the energy flux to smaller scales), then a fractional integration (i.e. a power law filtering) is used to model the turbulent velocity or passive scalar density field; the details are given in section 2. In the bounded cascade model, there is no conserved flux, the velocity or density fields are directly modeled with multiplicative cascades which are strongly "bounded" in order to obtain the necessary passive scalar statistics. In order to bound the cascade it is progressively and rapidly weakened at each step; as pointed out in [*Lovejoy & Schertzer*, 2006], this scale by scale bounding essentially kills off the intermittency so that the resulting field has the same scaling exponents as a truncated (non-intermittent, additive) gaussian process. Studies of radiative transport on the latter ([*Cahalan*, 1994], have unsurprisingly concluded that the effect of the horizontal cloud heterogeneity on the radiative transfer is small.

Finally, it is worth mentioning a related approach proposed by [*Davis, et al.*, 1999] to phenomenologically account for the cloud variability by replacing the standard exponential transmission (Green's) function by a power law corresponding to a Lévy flight model for photon paths. The justification is that cloud holes give rise to occasionally very long photon paths. While this model is interesting, it is not clear which – if any – cloud physical processes would give rise to Lévy flights. It is interesting to note that the multifractal cloud models discussed here do indeed give rise to quite long tailed distributions – but not "fat-tailed" (algebraic) ones such as in Lévy distributions. Although photon paths do exhibit clustering and other features of the Lévy walks (see Figs. 4 and 5), they in fact have finite variances. In addition, the Lévy flights correspond to "superdiffusion" in which, after N scatters, photons travel a distance N^s with $s = 1/\alpha > 1/2$ whereas – due to the trapping of photons in dense regions – we find $s < 1/2$ i.e. "subdiffusion" corresponding to a quite different phenomenology.

1.3 Transport in multifractal media

To date, all numerical studies of radiative transport in multifractal media have used the special Discrete Angle (DA) phase functions mentioned above and described in detail in section 2. In addition, for obvious reasons, they have concentrated almost exclusively on two dimensional systems (see however [*Gierens*, 1993], [*Gierens*, 1996a], [*Gierens*, 1996b], [*Borde & Isaka*, 1996]) with periodic horizontal boundary conditions and vertically incident radiation. Early studies were primarily numerical ([*Davis, et al.*, 1991], [*Davis, et al.*, 1993]) and aimed at demonstrating the potentially large effect of multifractal heterogeneity on the spatially averaged ("bulk effect") transport. For example, the latter papers found that for a cloud with strong intermittency ($C_1 = 1/2$, see section 2; c.f. realistic cloud values $C_1 \approx 0.1$), and mean optical thickness 100, the mean transmission is increased a factor of 3 with respect to the homogeneous counterpart. Similarly, [*Borde & Isaka*, 1996] numerically studied the statistical variation of mean cloud transmittances concentrating on the phase function and other parameters thought to be meteorologically most realistic. Since their clouds had relatively small effective optical thicknesses, the effect of the multifractality was not so large (the transfer problem becomes linear in the optically thin limit so that heterogeneity is no longer important).

More recent approaches have attempted to obtain more theoretical insight into the relation between the multifractal cloud and associated radiation fields. Based on the radiative transfer Green's function, [*Naud, et al.*, 1996] have argued that with respect to the cloud, the radiation is a kind of integration (presumably of fractional order). These authors showed that since multifractal fields are superimpositions of singularities of all orders, above a given critical value the effect of this integration is simply to shift all the singularities (below this value, they are smoothed out). Developing this idea further with the help of a novel statistical closure technique, [*Schertzer, et* *al.*, 1997] showed that the transfer is indeed an integral over the cloud but over a generally fractal flux tube. This gives a multifractal generalization of the Independent Pixel Approximation (IPA) often used to interpret satellite cloud radiances. Unfortunately this insight has not yet been followed up.

In this paper, we follow an approach based on the classical order of scattering method for solving the radiative transfer equation (the basis of the Monte Carlo solution method). The starting point is the exact calculation of single scattering statistics in multifractal clouds obtained by averaging the single scatter transmission function over the cloud statistics [*Lovejoy, et al.*, 1995], which produces a "mean field" type of result. This is used to justify a renormalization of the cloud, i.e. to replace the heterogeneous multifractal cloud by an "equivalent" thinner, homogeneous cloud. In the special multifractals (with analytic K(*q*), see below) considered in [*Davis, et al.*, 1993] this theoretically derived renormalization was shown to reproduce the numerical results and was very accurate even in optically thick clouds with high degrees of multiple scattering.

While these results were promising, they could not be directly applied to realistic clouds for several reasons. The first is that the cloud was assumed to be a conserved multifractal (a scale by scale energy flux). This means that the density fields are much rougher than those of (non-conserved) realistic clouds. The second is that realistic clouds have low density regions ("Levy holes") which are so frequent that their statistics are qualitatively different: negative moments diverge and the moment scaling function K(*q*) is a not analytic at the origin. This latter property is the source of serious (and interesting) technical difficulties discussed below. Both assumptions are at odds with cloud observations (see e.g. [*Tessier, et al.*, 1993], [*Sachs, et al.*, 2001], [Lovejoy, 2005 #826]). In this paper, we generalize these earlier results to lifting this restriction obtaining renormalization methods for realistic multifractal exponent functions. The key aspect remaining to be treated for realistic multifractal clouds, is the effect of scaling anisotropy especially for the vertical stratification which, according to recent lidar measurements ([*Lilley, et al.*, 2004]), is characterized by an "elliptical dimension" 2.55±0.02 (close to the theoretical value 23/9).

2. Single scattering in multifractal clouds

2.1 Multifractal cloud densities

In this section we derive the single scattering statistics through a multifractal cloud; the presentation is somewhat simplified and improved with respect to that of [*Lovejoy, et al.*, 1995] largely thanks to the systematic use of the Mellin transform.

As a model we take a cloud with a multifractal density field $\rho\left(\underline{x}\right)$ (in units such that $\langle\rho\rangle = 1$, $\underline{x} = (x, y, z)$) defined on a cloud having unit outer scale *L* = 1 in each dimension. Following basic turbulence phenomenology, we first define a (scale by scale) conservative multifractal φ_λ with the following ensemble averaged moments at scale ratio λ (λ ≥1 is the ratio of the largest cloud scale, set equal to one, over the scale of observation):

$$\left\langle \varphi_\lambda^q \right\rangle = \lambda^{K(q)} \tag{1}$$

where K(*q*) is the (convex) moment scaling function.

According to the usual turbulence phenomenology, the directly observable cloud density is related to the conserved flux φ by:

$$\rho_\lambda = \varphi_\lambda \lambda^{-H} \tag{2}$$

For example, according to Corrsin-Obukov ([*Corrsin*, 1951], [*Obukhov*, 1949]) theory of passive scalars, $\varphi = \chi^{3/2}\varepsilon^{-1/2}$, where χ is the passive scalar variance flux, ε is the energy flux and *H* = 1/3. In the horizontal, [*Lovejoy and Schertzer*, 1995], [Lilly et.al., 2004], have shown empirically that this is very close to the observations. Eq. (2) is essentially the result of dimensional analysis, the linear scaling factor λ^{-H} is interpreted statistically. In order to make a stochastic model of a field with the scaling statistics indicated in Eq. (2), the simplest procedure is to use the fractionally integrated flux (FIF) model ([*Schertzer & Lovejoy*, 1987]), in which it is interpreted as a fractional integration of order *H* (see section 4.8).

Mathematically, *K(q)* could be practically any convex function, so that multifractal modeling and analysis would require an unknown function, the equivalent of an infinite number of parameters. Fortunately, multifractal processes possess stable and attractive generators Γ_λ :

$$\Gamma_\lambda = \gamma_\alpha * \left|\underline{x}\right|^{-D/\alpha}$$
$$\varphi_\lambda = e^{\Gamma_\lambda} \tag{3}$$

11.5

where γ_α is a (white) Lévy noise subgenerator (of index α) and where "*" is the convolution operator ([*Schertzer & Lovejoy*, 1987]) and D is the dimension of space. The corresponding conservative multifractal process φ_λ is then characterized by only two parameters α and C_1:

$$K(q) = \frac{C_1}{\alpha - 1}\left(q^\alpha - q\right) \tag{4}$$

where $0 \le \alpha \le 2$ is the Lévy index of the generator (= log φ_λ; this is a Lévy process) and C_1 is the codimension of the mean, i.e. it is the codimension of the singularities which give the dominant contribution to the mean of the process (recall that the codimension of a set is the difference between the dimension of space in which the process is embedded and the dimension of that given set). When $\alpha = 2$, γ_α is a gaussian white noise and the "bare" φ_λ (i.e. the process cut-off at the finite resolution $1/\lambda$) is just a log-normal process. In this case, K(q) is quadratic, hence analytic. However, when $\alpha < 2$, the Lévy generator with its long algebraic tail completely changes the statistics and the phenomenology. In order for the moments $q > 0$ of φ_λ negative extremes; it must be an asymmetrical "extremal Lévy". The negative moments diverge due to the frequent large negative values of Γ. This leads to the presence of "Lévy holes" (see Figure 1) which are large low valued density regions; for radiative transfer, they are fundamental since they are relatively optically transparent.

NO SPACE

Figure 1: This figure shows a 500×500 pixel conservative ($H = 0$) multifractal cloud with $\alpha = 1.75$ and a relatively large intermittency parameter $C_1 = 0.3$ (the fractal dimension of the set giving the dominant contribution to the mean value is 2-0.3=1.7). Large density regions appear white, small density regions appear black. Note the presence of very large low valued density regions which are of fundamental importance because they are relatively optically transparent.

The above equations define the statistics of ρ via the moments; they can also be defined via their probability distributions:

$$\Pr\left(\varphi_\lambda > s\right) \sim \lambda^{-c(\gamma)}; \quad s = \lambda^\gamma \tag{5}$$

where "$\sim$" indicates equality to within slowly varying (e.g. logarithmic) factors. The moments and the probability densities are related by a Mellin transformation ([*Schertzer & Lovejoy*, 1992]; see Eq. (11) below); this reduces to a Legendre transformation ([*Parisi & Frisch*, 1985]) for the exponents:

$$\begin{aligned} c(\gamma) &= \max_q \left(q\gamma - K(q)\right) \\ K(q) &= \max_q \left(q\gamma - c(\gamma)\right) \end{aligned} \tag{6}$$

Eqs. (4) and (6) imply one to one relations between moments and singularities:

$$\gamma = K'(q); \quad q = c'(\gamma) \tag{7}$$

For universal multifractals,

$$\begin{aligned} c(\gamma) &= C_1\left(\frac{\gamma}{C_1\alpha'} + \frac{1}{\alpha}\right)^{\alpha'} \\ &= C_1\left(\frac{1}{\alpha} - \frac{\gamma}{\alpha\gamma_0} +\right)^{\alpha'}; \quad 0 \le \alpha < 1,\ 1 < \alpha \le 2 \end{aligned} \tag{8}$$

where: $\frac{1}{\alpha} + \frac{1}{\alpha'} = 1$ and $\gamma_0 = -C_1\frac{\alpha'}{\alpha} = -\frac{C_1}{\alpha - 1}$. It is valid for $\gamma > \gamma_0$ for $1 < \alpha < 2$ (= 0 otherwise) and for $\gamma < \gamma_0$ for $0 \le \alpha < 1$ (=0 otherwise). For $\alpha = 2$ the above is valid for all γ. From Eq. (8) we see that for $1 < \alpha \le 2$ γ_0 is the largest space filling (the codimension being 0) singularity. In addition, since for $1 < \alpha < 2$, $c'(\gamma_0) = 0$, we see that it is also the most probable and gives the dominant contribution to the zeroth order (q=0) cloud density moment.

Although real cloud fields are not conservative with H empirically close to the theoretical (Corrsin-Obukhov) passive scalar value 1/3, in the first part of this paper, and for the sake of simplicity, we restrict ourselves to the conservative case with universal multifractal parameters H = 0, $1 < \alpha \le 2$, and $0 \le C_1 \le 2$ (for the 2-D case). Whenever formulas are explicitly evaluated or graphical results displayed, we choose the values α = 1.75 and C_1 = 0.1, which approximate the parameters found in real clouds (see [*Lovejoy*, 2001], [*Lovejoy & Schertzer*, 2006]).

02.2 Cloud radiative properties

The extinction parameter κ is the scattering, absorption cross-section per unit mass of scattering media; it has dimensions of inverse distance. In the following, it will be convenient to nondimensionalize the distances by the overall system size L_{ext} (equivalent to considering a cloud of unit size), while simulttaneously nondimensionalizing κ by the same L_{ext}. It characterizes the strength of the matter-radiation coupling and is equal to the number of mean free paths across a homogeneous cloud having the same average desnity. In a cloud of unit size, let x be the physical length of a photon path. The optical path length is then defined as,

$$\tau(x) = \kappa \int_{\text{path}} \rho(\vec{r})\,dr \tag{9}$$

where the integration is over the straight line photon path of length x. The probability that a photon will travel a distance x without scattering is then given by the transmission function,

$$T = e^{-\tau}, \tag{10}$$

(known as "Beer's Law") and is the propagator from the radiative transfer equation. For "mean field" properties we require the statistical average of this quantity, the direct transmission, $\langle T(x)\rangle$, (where, for a fixed x, the average is to be taken over an ensemble of multifractal clouds), and the moments

$$\langle x^{q_p}\rangle = \int x^{q_p} p_x(x)\,dx, \tag{11}$$

where $p_x(x) = -\frac{\partial\langle T\rangle}{\partial x}$ is just the probability density for paths of length x.

The starting point is to write down an expression for the direct transmission

$$\langle T(x)\rangle = \int_0^\infty e^{-\tau} p_\tau(\tau)\,d\tau, \tag{12}$$

where $p_\tau(\tau)$ is the probability density for finding an optical path length as given by Eq. (9) and is a one-dimensional integral over a large scale factor $\lambda \equiv 1/x$ of a multifractal field that has been developed to some fine inner scale with scale ratio L; in other words, we start with an original multifractal with a high scale ratio $\Lambda \gg 1$ and spatially average to a smaller scale ratio λ. It is referred to as the "dressed field." Mathematically, the dressed field $\rho_{\lambda,d}$ at scale ratio $\lambda < \Lambda$ is:

$$\rho_{\lambda,d} = \lambda \int_{1/\lambda} \rho_\Lambda(x')\,dx' \tag{13}$$

For moments q below a critical value q_D, the bare and dressed statistics are the same to within factors of order unity: $\langle\rho^q_{\lambda,d}\rangle \approx \langle\rho^q_\lambda\rangle$. However for $q > q_D$ the former diverge while the latter remain finite [*Schertzer & Lovejoy*, 1987]. We assume here that $q < q_D$ so that it is acceptable to replace the dressed field by the bare field developed only down the scale λ, i.e. we take $\rho_{\lambda,d} \approx \rho_\lambda$. Defining τ_p as the (dimensionless) optical thickness through a physical distance x in a (random) cloud singularity γ, and recalling that for a multifractal field $\rho_\lambda = \lambda^\gamma$ with the singularities γ being an extremal Lévy random variable having probability density $p(\gamma)$, we find the following approximation:

$$\tau_p \approx \kappa\rho_\lambda x = \kappa\rho_\lambda \lambda^{-1} = \kappa\lambda^{\gamma-1}. \tag{14}$$

This "bare = dressed" approximation should be valid so long as x is small compared to 1 (the outer scale of the cloud): for small λ the bare field has undergone few cascade steps and therefore is less variable than the dressed field. In fact, the limit $\lambda \to 1$ is the uniform cloud, and serves as a useful check.

2.3 The direct transmission

We begin by finding an integral expression for $\langle T\rangle$ that can be evaluated. For technical reasons it is more convenient use the normalization of the probability density so as to rewrite Eq. (12) as

$$\langle T(x)\rangle = 1 - \int_0^\infty \left(1 - e^{-\tau}\right) p_\tau(\tau)\,d\tau \tag{15}$$

The problem now is that with the exception of the exponential part, Lévy probability densities are not expressible in closed form except in the special cases $\alpha = 1$ (Cauchy probability density function), $\alpha = 1/2$ ("inverse Gaussian"), and $\alpha = 2$ (Gaussian pdf). However, the Mellin transform of p_τ is straightforward so that with the help of the Parseval formula for products, we rewrite Eq. (15) in terms of the Mellin transformed quantities. We obtain an integral in the complex plane of the product of Mellin transforms (see, *e.g.* [*Bleistein & Handelsman*, 1986]).

$$\langle T\rangle = 1 - \frac{1}{2\pi i}\int_{r-i\infty}^{r+i\infty} M[1-e^{-\tau};-q]M[p_\tau;1+q]\,dq \tag{16}$$

with the Mellin transform and its inverse given by

$$M[f(\tau);q] \equiv \int_0^\infty \tau^{q-1} f(\tau)\,d\tau$$
$$f(\tau) = \frac{1}{2\pi i}\int_{c-i\infty}^{c+i\infty} \tau^{-q} M[f;q]\,dq. \tag{17}$$

The two Mellin transforms in equation (16) can be evaluated:

$$M[1-e^{-\tau};-q] = -\Gamma(-q)$$
$$M[p_\tau(\tau);1+q] = \kappa^q x^{q-K(q)} \tag{18}$$

The first transform is a standard result. The second arises from the definition of the moment scaling function $K(q)$ (Eq. (4) with $x=\lambda^{-1}$). We therefore arrive at an essential expression,

$$\langle T(x)\rangle = 1+\frac{1}{2\pi i}\int_{\substack{r-i\infty\\0<r<1}}^{r+i\infty}\kappa^{q}x^{q-K(q)}\Gamma(-q)\,dq \quad . \tag{19}$$

The integration is along a vertical path which lies in the common strip of analyticity of the two Mellin transforms. While this does not at first seem like a simplification, it will provide a useful tool in finding asymptotic expansions for the photon path moments. Moreover it can be easily integrated numerically, as shown in Figure 2.

NO SPACE

Figure 2: $\ln\langle T\rangle$ vs. x (numerical integration). Here $\kappa=100$. For path lengths less than x_c, the mean transmission is essentially exponential at some reduced value

Two observations are in order. The first is that the direct transmission through a cloud with a large variability in scatterers density can be much greater than for a uniform cloud of the same κ. The second is that there are at least two main regimes: a short-distance regime in which the transmission is approximately exponential at some reduced value of κ, and a long-distance regime in which the transmission falls off more gradually.

2.4 The singularity formalism for single scattering

We have seen that in multifractals for large λ, the probability and moment descriptions are simply related through a Legendre transformation (Eq. (6)). [*Lovejoy, et al.*, 1995] showed that for large κ an analogous set of exponents and relations exist for the radiative transfer. First, define the (random) "scattering singularity" γ_p for the random optical distance traversed by a photon before scattering:

$$\tau_p=\kappa^{\gamma_p} \tag{20}$$

Now, we interpret the mean transmittance $\langle T\rangle$ as the probability distribution of the random photon scattering distances:

$$\langle T\rangle = \Pr\left(\tau_p>\kappa^{\gamma_p}\right)\sim\kappa^{-c_p(\gamma_p)} \tag{21}$$

We now use,

$$x=\tau_p/\kappa=\kappa^{\gamma_p-1} \tag{22}$$

and insert this into Eq. (19):

$$\kappa^{-c_p(\gamma_p)} = 1+\frac{1}{2\pi i}\int_{\substack{r-i\infty\\0<r<1}}^{r+i\infty}\kappa^{q\gamma_p-K(q)(\gamma_p-1)}\Gamma(-q)\,dq \quad . \tag{23}$$

If we now assume that $K(q)$ is analytic at the origin, we can take r to the left (past the pole in $\Gamma(-q)$ at the origin); this residue contributes a value -1 which cancels the one in Eq.(23) to yield

$$\kappa^{-c_p(\gamma_p)} = \frac{1}{2\pi i}\int_{\substack{r-i\infty\\r<0}}^{r+i\infty}\kappa^{q\gamma_p-K(q)(\gamma_p-1)}\Gamma(-q)\,dq \tag{24}$$

Note that the assumption of analyticity at the origin is valid for many popular multifractal models such as the log-Poisson model ([*She and Levesque*, 1994]) or the "*p* model" ([*Meneveau and Sreenivasan*, 1987]) but is invalid for all the universal multifractals except the special "lognormal" multifractal $\alpha=2$ (see [*Lovejoy,et.al.*, 1995] for the latter); the cases $\alpha<2$ have a branch cut along the negative real axis ending at the origin. The final step is to make a transformation of variables and define the photon moment exponent $K_p(q_p)$,

$$\begin{aligned} q_p &= K(q)-q \\ K_p(q_p) &= K(q) \end{aligned} \tag{25}$$

to obtain:

$$\kappa^{-c_p(\gamma_p)} \sim \int_{-\infty}^{0}\kappa^{-q_p\gamma_p+K_p(q_p)}\,f(q_p)\,dq_p \tag{26}$$

where we have deformed the limits of integration to lie on the negative q_p axis. f is an unimportant sub-exponential function (see [*Lovejoy, et al.*, 1995]). If $K(q)$ and hence $K_p(q_p)$ have unique minima (recall, they are convex), and since $K(0)=K(1)=0$, if $K(q)$ is real for $q<0$, then this minimum occurs for real $q_p<0$; it will lie on the domain of integration above. In that case, the "moving maximum" method of asymptotic approximation (c.f.

11.5

[*Bender and Orszag,* 1978]) allows us to conclude that for large enough κ :

$$\begin{aligned} c_p\left(\gamma_p\right) &= \max_q\left(q_p\gamma_p - K_p\left(q_p\right)\right) \\ K_p\left(q_p\right) &= \max_q\left(q_p\gamma_p - c_p\left(\gamma_p\right)\right) \end{aligned} \tag{27}$$

The final formula relating cloud and scattering exponents follows by inverting the transform; we see for example that:

$$\left\langle \tau_p^{q_p} \right\rangle = \kappa^{K_p\left(q_p\right)} = \kappa^{q_p}\left\langle x^{q_p} \right\rangle \tag{28}$$

The Legendre pairs in Eqs. (6) and (27) allow us to associate unique singularities with moments:

$$\begin{aligned} \gamma &= K'\left(q\right) = \frac{dq_p}{dq} + 1 \\ \gamma_p &= K_p'\left(q_p\right) = \frac{dq}{dq_p} + 1 \end{aligned} \tag{29}$$

from which we derive,

$$\left(\gamma - 1\right)\left(\gamma_p - 1\right) = 1 \tag{30}$$

Eqs. (15), (20), (21), (22) and (24) (which are only exact in the limit $\kappa > \lambda \to \infty$) establish one to one relations between cloud densities and statistics, and photon paths and statistics; these will be quite helpful in interpreting the results below. These relationships between exponents are only between values which give dominant contributions to integrals; they are only exact in the limit of large λ , large κ . For example, using Eq. (30) we see that the most probable cloud density singularity, $\gamma_0 = -\frac{C_1}{\alpha - 1}$, corresponds to the photon scattering singularity:

$$\gamma_{p0} = 1 - a \qquad ; a = \frac{1}{1-\gamma_0} = \left(1 + \frac{C_1}{\alpha - 1}\right)^{-1} \tag{31}$$

is the exponent for the photon distance x that will play a fundamental role in later developments. Since we saw γ_0 dominates the moment $q = 0$, and $q_p = K(q) - q$ we see that γ_{p0} gives the dominant contribution to $q_p = 0$, and finally, this shows that $c_p'(\gamma_{p0}) = q_p(\gamma_{p0}) = 0$ so that γ_{p0} is in fact the most probable photon scattering singularity. In the case $\alpha = 2$, [*Lovejoy, et al.*, 1995] show:

$$\begin{aligned} c_p\left(\gamma_p\right) &= \frac{\left(1-\left(1+C_1\right)\left(1-\gamma_p\right)\right)^2}{4C_1\left(1-\gamma_p\right)} \\ K_p\left(q_p\right) &= q_p - \frac{\sqrt{\left(1+C_1\right)^2 + 4C_1 q_p} - \left(1+C_1\right)}{2C_1} \end{aligned} \tag{32}$$

In the following section, we show how this formalism can be extended to the case $1 < \alpha < 2$ and show the corresponding graphs of K_p , c_p .

3. Single Scattering Direct Transmission and Moments for $1 < \alpha < 2$

3.1 The transmission function

The idea of two scattering regimes is more than apparent. For the special value of photon path length x_0 (corresponding to the most probable path length singularity γ_{p0}):

$$x = x_0 = \kappa^{1-\gamma_{p0}} = \kappa^{-a} = \kappa^{-\left(1+\frac{C_1}{\alpha-1}\right)^{-1}} \tag{33}$$

which might be called the renormalized *scattering length*. Eq.(19) is practically stationary with respect to a change in κ (see Figure 3).

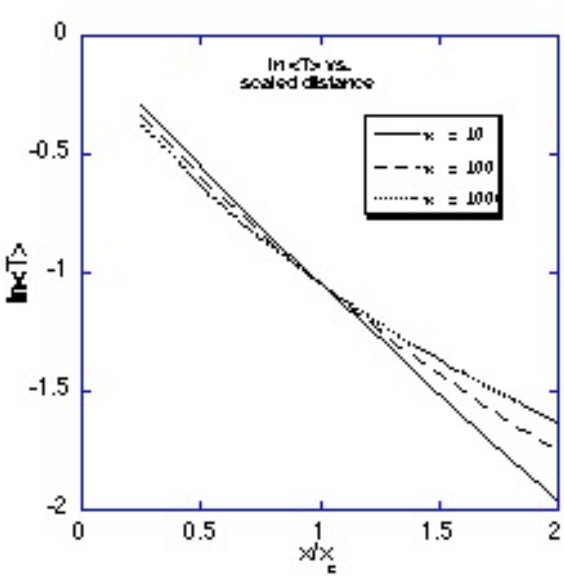

11.5

Figure 3. $\ln\langle T\rangle$ vs. scaled distance x/x_c (numerical integration). solid line κ =10, dashed line κ =100, dottted line κ =1000.

This behavior can be traced to the fact that the linear term in the exponent of the integrand of Eq. (19) vanishes at x_0 leaving,

$$\left\langle T\left(x_c\right)\right\rangle = 1+\frac{1}{2\pi i}\int_{r-i\infty}^{r+i\infty}\kappa^{\gamma_{p0}q^{\alpha}}\Gamma(-q)\,dq \approx e^{-1} \qquad (34)$$

The simplification comes about by choosing an integration path with $r\approx 0$ so that $\kappa^{\gamma_{p0}q^{\alpha}}\approx 1$ over the range where the gamma function is makes its major contribution. We then apply the inverse Mellin transform of Eq.(17) (this argument does not work for α<1). The approximation is borne out by the numerics in Figure 3. Since the transmission function falls to 1/*e* at x_0 it is easy to see that a good approximation for the transmission in the short distance regime is given by

$$\langle T\rangle \approx e^{-\kappa_{eff}x},\ \ x<x_0;$$
$$\kappa_{eff}=x_0^{-1}=\kappa^{a}=\kappa^{\left(1+\frac{C_1}{\alpha-1}\right)^{-1}}. \qquad (35)$$

The approximation of Eq. (35) is plotted in Figure 2 and is a central result: for single scatterings the transmission is essentially exponential but with a reduced or renormalized extinction coefficient. More justification of this will be given later, Figs. 4 and 5 show the implications for photon path distributions. Another way of thinking about this is that $\langle T\rangle$ is determined almost entirely for short distances by the most probable singularity in the density field.

NO SPACE

Fig. 4: This shows part of a random photon path using the derived distribution assuming each step is statistically independent ($\kappa=1000$). Although the walk appears very similar to a Lévy flight (notice the clusters within clusters), the variance is in fact finite, the walk with independent steps will eventually tend to the standard gaussian brownian motion limit. The clustering is in fact due to the sharp difference in the statistics of short and long steps ($x<x_0$, $x>x_0$ respectively). In section 4 we see that even for large numbers of steps, they are not independent due to the long range correlations in the multifractal cloud (Fig. 5).

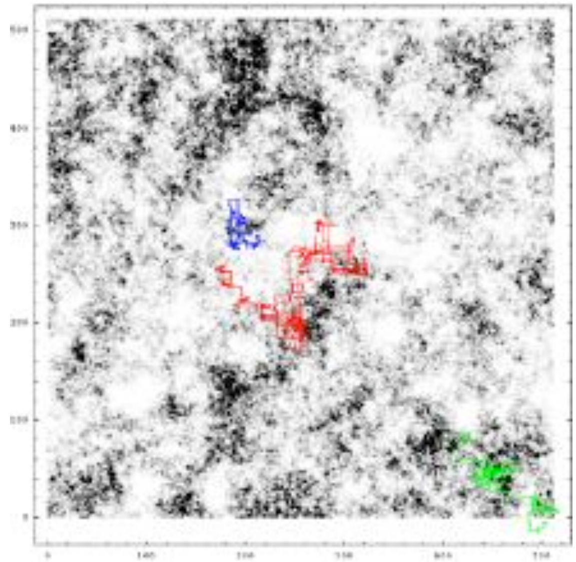

Fig. 5: Three photons paths, 100 scatters each on a conservative multifractal cloud (2-*D*), with α=1.75, C_1=0.1. We also see clustering when the photon moves into dense cloud regions. The cloud (and path) are periodic. Note here, discrete angle phase functions were used, isotropic in the four orthogonal directions.

3.2 The photon moment statistics: the power law term (36)

We turn our attention now to the path length moments,

$$\left\langle x^{q_p}\right\rangle = \int_0^1 x^{q_p}p_x\left(x\right)dx = -\int_0^1 x^{q_p}\frac{\partial\langle T\rangle}{\partial x}dx \qquad (37)$$

Recall that the upper limit here is not infinity because the cloud has an outer scale of $x=1$. Integrating by parts we get,

$$\left\langle x^{q_p}\right\rangle = -x^{q_p}\langle T\rangle\Big|_0^1 + \int_0^1 q_p x^{q_p-1}\langle T\rangle\,dx \qquad (38)$$

The boundary term evaluates to $e^{-\kappa}$; it can be ignored for large κ . After substituting our integral expression for $\langle T\rangle$ we arrive at,

$$\left\langle x^{q_p}\right\rangle = 1-e^{-\kappa}+W(q_p)$$
$$W(q_p)\equiv\frac{q_p}{2\pi i}\int_0^1 x^{q_p-1}\int_{\substack{r-i\infty\\0<r<1}}^{r+i\infty}\kappa^{q}x^{q-K(q)}\Gamma(-q)\,dq\,dx \qquad (39)$$

The order of integration may be reversed, justified on grounds of uniform convergence. The integral with respect to x is elementary giving

11.5

$$W(q_p) = \frac{q_p}{2\pi i} \int_{\substack{r-i\infty \\ 0<r<1}}^{r+i\infty} \frac{\kappa^q \Gamma(-q)}{q_p + q - K(q)} dq \qquad (40)$$

An analysis of Eq. (40) depends critically on the properties of the moment scaling function *K(q)*, which determines the locations of the poles of the integrand. For conservative multifractals, *K(q)*is a concave upward function with *K(0)=K(1)=0* as shown in Fig. 6.

NO SPACE

Fig. 6: $\mathrm{K}(q)$ vs. q . The location of the poles in the integrand of Eq. (40) are given by the solution of $q_p + q = \mathrm{K}(q)$.

It is obvious from the figure that there will always be one real root of

$$q_p + q = K(q)\,, \qquad (41)$$

within $0 \le q_- < 1$ for $-1 < q_p \le 0$ so that the condition on the integration path in Eq. (40) can be satisfied by taking $q_- < r < 1$. We also see that the condition can never be satisfied for $q_p \le -1$; in other words, these photon path moments diverge. If *K(q)* is analytic (as is shown in the figure), then the positive moments can be handled with no modification. When *K(q)* is given by Eq. (4) with $\alpha < 2$, however, *K(q)*has a branch cut along the negative *q*-axis and q_- will be complex and multiple–valued. In any event, so long as $-1 \le q_p$ Eq. (40) is applicable.

It is important to appreciate that although Eq. (41) relating *q*, q_p, and *K(q)* is the same as that obtained for analytic *K(q)* relating dominant exponents, here, the relation determines the positions of poles in a complex integral. In this way, the relation continues to be important even when the exponential is not dominant (as we shall see for 1<α<2 below). See Figures 7 and 8.

When *K(q)*is analytic, the evaluation of Eq. (40) is straightforward, especially if the two roots can be obtained in closed form. The case for $\alpha=2$ is given in Eq. (32).

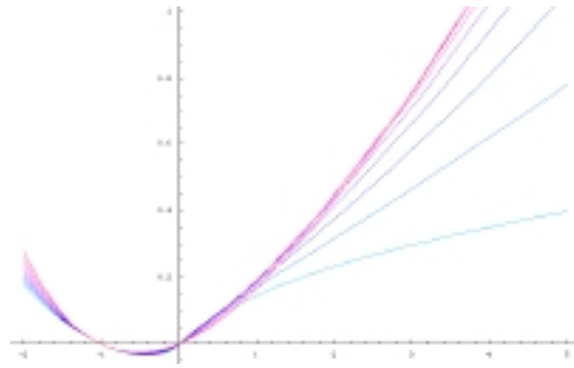

Fig. 7: $\mathrm{K}_p(q_p)$ as a function of q_p obtained numerically using the Eq. (25); all curves have $C_1 = 0.1$, from bottom to top, $\alpha = 1.1$ to 1.9 in steps of 0.1. Curves for other C_1 values are obtained using the fact that $\mathrm{K}(q)/C_1 = \mathrm{K}_p(q_p)/C_1$ is independent of C_1.

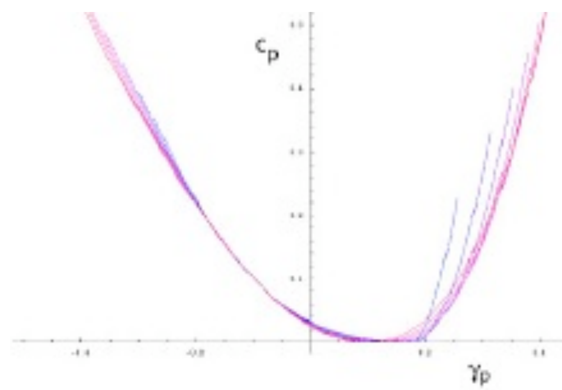

Fig. 8: $c_p(\gamma_p)$: Obtained by numerical Legendre transformation of the above. Here we have α=1.3 to 1.9 (bottom to top).

3.3 The photon moment statistics: the logarithmic terms

We have seen that the poles will give us power law terms. Space limitations prevent us from giving a complete analysis of the logarithmic terms. We present only a summary of the results and leave the details for a future paper.

For positive and negative moments the first three terms in the asymptotic expansion are

11.5

$$\left\langle x^{q_p}\right\rangle \sim \Gamma(1+aq_p)\kappa^{-aq_p}+B\left(\log\kappa\right)^{-\alpha}+C\left(\log\kappa\right)^{-(\alpha+1)}$$
$$B=\frac{C_1}{q_p\Gamma(2-\alpha)}$$
$$C=\left(\frac{\gamma_E\gamma_0}{q_p}-\frac{2\gamma_0(1-\gamma_0)}{q_p{}^2}\right)\frac{1}{\Gamma(-\alpha)},\quad \gamma_0=\frac{-C_1}{\alpha-1}$$
$$a=\left(1+\frac{C_1}{\alpha-1}\right)^{-1} \tag{42}$$

Note that the two logarithmic terms vanish for α=2. For large κ it is the first (algebraic) term which dominates the negative moments since *q(q$_p$)* is positive. This expression will be applicable to both positive *and* negative moments, the only distinction being that the algebraic and logarithmic terms trade places in importance as q_p changes sign. Once again, we have seen that the statistics of short pathlengths (which are described by the negative q_p) differ from the long pathlength (described by the positive q_p). This is not really surprising since the Lévy probability density for the density singularities is maximally asymmetric, except, of course, for the symmetric Gaussian case of $\alpha=2$. But for this exception the logarithmic terms vanish so the moment function is always algebraic, a result that obtains whenever *K(q)* is analytic. Fig. 9 shows that the above approximations are indeed quite accurate for q_p=2.

NO SPACE

Fig. 9: For α=1.75, C_1=0.1, we show ln<x^2> versus $\log_{10}\kappa$ The heavy solid line gives the numerical integration of eq. (40). The thin solid lines indicate the first term (exponential) and second (logarithmic) terms respectively of eq.(42). The dashed line shows the improvement when the third term of eq. (42) is included.

4. Multiple scattering

4.1 Discussion

From the point of view of applications, the above results have severe limitations. First, it is not obvious how the above single scattering calculations are relevant to multiple scattered radiation in thick clouds. In addition, even for single scattering, it is not clear that the results will be relevant in non conservative clouds in which the cloud density is related to the (scale by scale) conservative multifractal fluxes by a fractional integration i.e.:

$$\rho\left(\underline{x}\right)=\phi\left(\underline{x}\right)*\left|\underline{x}\right|^{-(D-H)} \tag{43}$$

where ϕ is a flux and "*" denotes "convolution" and *D* is the dimension of space. For example the Corrsin-Obukov law for passive scalar advection yields *H*=1/3 and $\phi=\chi^{1/2}\varepsilon^{-1/6}$ where χ is the passive scalar variance flux and ε is the energy flux. Observations ([*Lilley, et al.*, 2004], [*Lovejoy and Schertzer*, 1995]) show that in the horizontal *H* is indeed close to 1/3. Unfortunately, the analytic treatment of the statistics of the above FIF model with *H*≠0 is too difficult; the same is true of extending the above directly to multiple scattering since successive scatters are strongly correlated.

In order to study both multiple scattering and the effect of *H*>0, we therefore turn to numerical techniques. Probably the simplest technique of all is the Monte Carlo technique which is indeed quite standard for radiative transfer calculations. In this technique, photons are simulated and statistics are built up from many virtual photons. Considering pure scattering (no absorption), after starting the photon off at a boundary in the direction of incident radiation, it propagates in a straight line until the total integrated optical thickness equals an exponential random deviate (this comes from the standard exponential propagator/Green's function, $e^{-\tau}$). The direction of the photon is then changed randomly according to the scattering phase function. Fig. (14) immediately shows the difficulty in applying single scattering results; the successive scatters never completely decorrelate; rather than obtaining a standard linear law of variance growth with number of scatters N, one obtains an anomalous law:

$$\left\langle x^2\right\rangle \propto N^a \tag{44}$$

with a given by Eq.(42). One can also see from the figure that the *N*=1 result of single scattering theory is above the asymptotic line so that clearly the multiple scattering cannot be obtained trivially from the single scattering result. We can already note that if we define the "effective" number of scatters as $N_a=N^a$, then we recover the classical homogeneous medium result for N_a. The result of Eq. (47) shows that the fractal dimension D_f of the photon path (e.g. in fig. 5) is:

$$D_f=2/a=2+\frac{2C_1}{\alpha-1} \tag{45}$$

which fills the plane (since 0 < *a* < 1 and C_1 > 0).

11.5

Although we do not give more than numerical justification for this result, we note that for α=2 (the log-normal multifractal), a=1/(1+C_1) which is identical to the exponent for 1-D diffusion in that case ([*Lovejoy, et al.*, 1998]). What is curious is that the 1-D diffusion result does not continue to be valid in 2-D ([*Marguerite, et al.*, 1997]), whereas fig. 10 shows that the 1-D diffusion result holds for 2-D radiative transfer. The difference is presumably in the nature of the "trapping" of random walking particles.

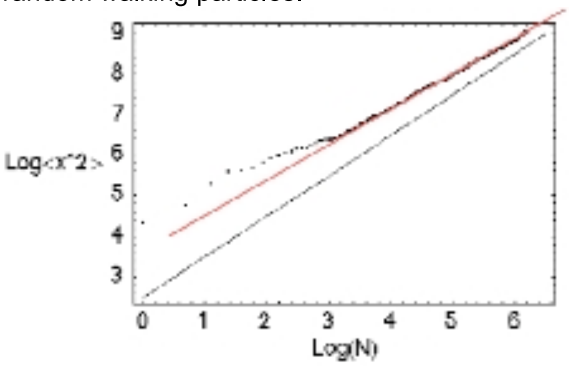

Fig. 10: This shows $ln\langle x^2\rangle$ vs. lnN for α=1.75, C_1=0, κ=512; the largest rms distance (measured in pixels) corresponds to 90 pixels. The orange line is N^a where a is the theoretical exponent (eq. 0.44) = 0.882 here; the black line is the classical linear variance law. Since a<1, we have "subdiffusion.

5. CONCLUSION

We showed how our earlier single scattering theory 1) can be extended to non-conservative (*H>0*) general "universal" multifractal clouds, and 2) how the analytic single-scattering results can be generalized to multiple-scattering. Indeed, the theoretical and numerical single scattering analytic results give accurate predictions for the mean cloud optical properties of clouds with realistic multifractal parameters and cloud optical thicknesses. By varying the extinction coefficient, we are able to study the effect of increasing cloud thickness, for typical cloud mean optical thickness in the range 8-100. For example, using the observed multifractal cloud characteristics, we predict that the mean cloud transmission decreases with the 0.88 power of the total optical thickness (the corresponding homogeneous exponent being unity). For clouds with a total optical thickness of 100 (with 1 - g = 0.15) this is a non-negligible 30-40% effect with respect to homogeneity.

REFERENCES:

Acker, A., K. Gesicki, Y. Grosdidier, S. Durand (2002), Turbulent planetary nebulae around [WC]-type stars, *Astronomy and Astrophysics*, v.384, pp.620-628

Barker, H. W., and J. A. Davies (1992), Cumulus cloud radiative properties and the characteristics of satellite radiance wavenumber spectra, *Remote Sens. Environ.*, *42*, 51-64.

Bazell, D., & F. X. Désert (1988), *The Astrophysical Journal*, 333, 353

Beech, M. (1992), *Astrophysics & Space Sciences*, 192, 103

Blacher, S., & J. Perdang, J. (1990), *Vistas in Astronomy*, 33, 393

Bleistein, N., and R. A. Handelsman (1986), *Asymptotic Expansions of Integrals*, Dover, Mineola.

Borde, R., and H. Isaka (1996), Radiative transfer in multifractal clouds, *J. Geophys. Res.*, *101*, 29,461-429,478.

Bouchaud, J. P., and A. Georges (1990), Anomalous diffusion in disordered media: statistical mechanisms, models and physics applications, *Phys. Reports*, *195*, 127-293.

Brunt, C. M., M. H. Heyer (2002), *The Astrophysical Journal*, 566, 289

Busygin, V. P., et al. (1973), Optical properties of cumulus clouds and radiant fluxes for cumulus cloud cover, *Izv. Acad. Sci. USSR Atmos. Oceanic Phys.*, *9*, 1142-1151.

Cahalan, R. (1994), Bounded cascade clouds: albedo and effective thickness, *Nonlin. Proc. in Geophys.*, *1*, 156-167.

Cahalan, R. F. (1989), Overview of fractal clouds, in *Advances in Remote Sensing Retrieval Methods*, edited by A. Deepak, et al., A. Deepak, Hampton Va.

Cahalan, R. F., et al. (1994), The albedo of fractal stratocumulus clouds, *J. Atmos. Sci.*, *51*, 2434-2455.

Chandrasekhar, S., Radiative Transfer (1950, Clarendon Press, Oxford; reprinted by Dover Publications, Inc., 1960)

Corrsin, S. (1951), On the spectrum of Isotropic Temperature Fluctuations in an isotropic Turbulence, *Journal of Applied Physics*, *22*, 469-473.

Davis, A., et al. (1990), Discrete Angle Radiative Transfer. Part III: numerical results on homogeneous and fractal clouds, *Journal of Geophysical Research*, *95*, 11729-11742.

Davis, A., et al. (1991), Radiative transfer in multifractal media, paper presented at SPIE.

Davis, A., et al. (1993), Supercomputer simulation of radiative transfer inside multifractal cloud models, in *International Radiation Symposium 92*, edited by A. A. e. al, pp. 112-115, Deepak, Hampton, Virginia.

Davis, A. B., et al. (1999), Anomalous/Levy photon diffusion theory: toward a new parametrisation of shortwave transport in c
loudy columns, paper presented at Ninth ARM Science Team meeting, US Dept. of Energy, San Antonio Texas, March 22-26.

Falgarone, E., T. G. Phillips, C. K. Walker (1991), *The Astrophysical Journal*, 378, 186

Falgarone, E., P. Hily-Blant, F. Levrier (2004), *Astrophysics & Space Sciences*, 292, 89

Fleck, R. C. (1996), *The Astrophysical Journal*, 458, 739

Gabriel, P., et al. (1990), Discrete Angle Radiative Transfer. Part II: renormalization approach to scaling clouds, *Journal of Geophysical Research*, *95*, 11717-11728.

Gabriel, P., et al. (1988), Multifractal Analysis of resolution dependence in satellite imagery, *Geophys. Res. Lett.*, *15*, 1373-1376.

Gabriel, P., S. Lovejoy, D. Schertzer, G.L. Austin (1986), Radiative transfer in extremely variable fractal clouds, paper presented at 6th conference on atmospheric radiation, Amer. Meteor. Soc., Boston, Williamsburg, Va.

11.5

Gierens, K. M. (1993), A fast six-flux radiative transfer method for application in finite cloud models, *Beitr. Phys. Atmosph., **66**,* 73-87

Gierens, K. M. (1996a), Simplification of the discrete angle radiative transfer method for clouds with translational symmetry, *Beitr. Phys. Atmosph., **69**,* 355-357

Gierens, K. M. (1996b), Numerical simulation of persistent contrails, *J. Atmos. Sci., **53***, 3333-3348

Gill, A. G., & R. H. Henriksen (1990), *The Astrophysical Journal Letters*, 365, L27

Grosdidier, Y. & A. Acker (2004), Mass-loss in central stars of planetary nebulae and in Wolf-Rayet stars, in EAS Publications Series, Volume 13, 2004, *Evolution of Massive Stars, Mass Loss and Winds*, held in Aussois and Oléron, France, October 13-18, 2002 and October 6-10, 2003. Edited by M. Heydari-Malayeri, Ph. Stee and J.-P. Zahn, pp.317-337

Havlin, S., and D. Ben-Avraham (1987), Diffusion in disordered media, *Adv. Phys.*, ***36***, 695-798.

Lane-Veron, D. E., and R. C. Somerville (2004), Stochastic theory of radiative transfer through generalized cloud fields, *J. Geophys. Res.*, *109*, D18113.

Lilley, M., et al. (2004), 23/9 dimensional anisotropic scaling of passive

admixtures using lidar aerosol data, *Phys. Rev. E*, *70*, 036307-036301-036307.

Lovejoy, S., et al. (1995), Scattering in multifractal media., paper presented at Particle Transport in Stochastic Media, American Nuclear Society, Portland, Or.

Lovejoy, S., D. Schertzer (1989), Fractal clouds with Discrete Angle Radiative transfer, in *Inter. Rad. Symp. 88*, edited by J. F. G. C. Lenoble, pp. 99-102, Deepak.

Lovejoy, S., et al. (1990), Discrete Angle Radiative Transfer. Part I: scaling and similarity, universality and diffusion, *Journal of Geophysical Research*, *95*, 11699-11715.

Lovejoy, S., and D. Schertzer (1990), Multifractals, Universality classes and satellite and radar measurements of cloud and rain fields, *Journal of Geophysical Research*, *95*, 2021.

Lovejoy, S., and D. Schertzer (1995), How bright is the coast of Brittany? in *Fractals in Geoscience and Remote Sensing*, edited by G. Wilkinson, pp. 102-151, Office for Official Publications of the European Communities, Luxembourg.

Lovejoy, S., and D. Schertzer (2004), Multifractals, cloud radiances and rain, *J. Hydrol.*, *(in press).*

Lovejoy, S., and D. Schertzer (2005), Multifractal cloud radiances, rain and multifractal models, *J. of Hydrol.*, *(in press)*.

Lovejoy, S., et al. (1998), Diffusion on one dimensional multifractals, *Water Res. Res.*, *34*, 3283-3291.

Lovejoy, S., et al. (1993), Radiative Transfer and Multifractal Clouds: theory and applications, in *I.R.S. 92*, edited by A. A. e. al, pp. 108-111.

Lovejoy, S., Schertzer, D., Stanway, J. D. (2001), Direct Evidence of planetary scale atmospheric cascade dynamics, *Phys. Rev. Lett.*, *86*, 5200-5203.

Marguerite, C., et al. (1997), Copepod diffusion within multifractal phytoplankton fields, *J. Marine Biol.*, *(in press)*.

McKee, T., and S. K. Cox (1976), Simulated radiance patterns for finite cubic clouds, *J. Atmos. Sci*, *33*, 2014- 2020.

Meakin, P. (1987), Random walks on multifractal lattices, *J. Phys. A*, ***20***, L771-L777.

Meneveau, C., and K. R. Sreenivasan (1987), Simple multifractal cascade model for fully develop turbulence, *Physical Review Letter*, *59*, 1424-1427.

Miesch, M. S., & J. Bally (1994), *The Astrophysical Journal*, 429, 645

Naud, C., et al. (1996), Fractional Integration and radiative transfer in multifractal atmospheres, in *Stochastic Models in Geosystems*, edited by W. Woyczynski and S. Molchansov, pp. 239-267, Springer-Verlag, New York.

Obukhov, A. (1949), Structure of the temperature field in a turbulent flow, *Izv. Akad. Nauk. SSSR. Ser. Geogr. I Geofiz*, *13*, 55-69.

Olver, F. W. J. (1974), *Asymptotics and Special Functions*, Academic, New York. p. 120

Parisi, G., and U. Frisch (1985), A multifractal model of intermittency, in *Turbulence and predictability in geophysical fluid dynamics and climate dynamics*, edited by M. Ghil, et al., pp. 84-88, North Holland, Amsterdam.

Preisendorfer, R. W., and G. I. Stephens (1984), Multimode radiative transfer in finite optical media, I fundamentals, *J. Atmos. Sci.*, *41*, 709-724.

Sachs, D., et al. (2001), The multifractal scaling of cloud radiances from 1m to 1km, *Fractals*, *in press*.

Schertzer, D., and S. Lovejoy (1987), Physical modeling and Analysis of Rain and Clouds by Anisotropic Scaling of Multiplicative Processes, *Journal of Geophysical Research*, *92*, 9693-9714.

Schertzer, D., and S. Lovejoy (1992), Hard and Soft Multifractal processes, *Physica A*, *185*, 187-194.

Schertzer, D., et al. (1997), New developments and old questions in multifractal cloud modeling, satellite retrievals and anomalous absorption, paper presented at 7th Atmos. Rad. Meas. (ARM) meeting, San Antonio.

Schuster, A. (1905), Radiation through a foggy atmosphere, The Astrophysical Journal, 21, pp. 1-22

She, Z., S., and E. Levesque (1994), *Phys. Rev. Lett.*, *72*, 336.

Tessier, Y., et al. (1993), Universal Multifractals: theory and observations for rain and clouds, *Journal of Applied Meteorology*, *32*, 223-250.

Weinman, J. A., and P. N. Swartzrauber (1968), Albedo of a striated medium of isotrpically scattering particles, *J. Atmos. Sci.*, *25*, 497-501.

Weissman, H., S. Havlin (1988), Dynamics in multiplicative processes, *Phys. Rev. B*, *37*, 5994-5996.

Welch, R. M., et al. (1980), *Solar radiation and clouds*.

Witt, A. N. & K. D., Gordon (1996), Multiple Scattering in Clumpy Media. I. Escape of Stellar Radiation from a Clumpy Scattering Environment, *The Astrophysical Journal,* v.463, pp. 681-693.

Witt, A. N. & K. D., Gordon (2000), Multiple Scattering in Clumpy Media. II. Galactic Environments, *The Astrophysical Journal*, v. 528, pp. 799-816.

Varosi, F. & E., Dwek (1997), Radiative Transfer in Clumpy and Fractal Media, in *The Ultraviolet Universe at Low and High Redshift : Probing the Progress of Galaxy Evolution : College Park, MD May 1997.* Edited by William H. Waller [et al.]. New York : American Institute of Physics, 1997. Also *AIP Conference Proceedings, v.408.,* p.370.

Juvela, M. (1997), Non-LTE radiative transfer in clumpy molecular clouds, *Astronomy and Astrophysics*, v.322, pp.943-961